

Machine Learning Models for Accurately Predicting Properties of CsPbCl₃ Perovskite Quantum Dots

Mehmet Sıddık Çadircı^{1*}, Musa Çadircı²

¹ *Faculty of Science, Department of Statistics, Cumhuriyet University, Sivas, Turkey.*

² *Department of Electrical & Electronics Engineering, Duzce University, Düzce, Turkey.*

* **Corresponding author, Email:**msiddikcadirci@cumhuriyet.edu.tr

Abstract

Perovskite Quantum Dots (PQDs) have a promising future for several applications due to their unique properties. This study investigates the effectiveness of Machine Learning (ML) in predicting the size, absorbance (1S abs) and photoluminescence (PL) properties of CsPbCl₃ PQDs using synthesizing features as the input dataset. the study employed ML models of Support Vector Regression (SVR), Nearest Neighbour Distance (NND), Random Forest (RF), Gradient Boosting Machine (GBM), Decision Tree (DT) and Deep Learning (DL). Although all models performed highly accurate results, SVR and NND demonstrated the best accurate property prediction by achieving excellent performance on the test and training datasets, with high R² and low Root Mean Squared Error (RMSE) and low Mean Absolute Error (MAE) metric values. Given that ML is becoming more superior, its ability to understand the QDs field could prove invaluable to shape the future of nanomaterials designing.

1 INTRODUCTION

Within computer science, artificial intelligence (AI) refers to the study of designing intelligent machines which can sense the environment around them and take appropriate actions accordingly [15]. Machine learning (ML) is a branch of artificial intelligence that employs algorithms to develop mathematical models from data for solving specific problems directly without applying physical principles that gave birth to the data. This method is especially valuable when the connection between the variables used in the study and the results of the study is not understood. Widespread access to computational power along with the increasing amount of data available for experimentation has resulted in the emergence and application in different areas of science and industry of advanced machine learning models [8, 19]. Thanks to the capability of evaluating the massive amount of data, Machine learning (ML) is significant for predicting

QDs' properties with a high accuracy. Since QDs' properties are highly dependent on the size, and composition[4], ML algorithms are appropriate tools to handle the data and exhibit well-expressed interactions between the input variables and the resultant properties. Moreover, ML can improve the procedure of synthesizing QDs in order to give out desired characteristics without running more expensive tests and complex simulations which take much time[20]. Besides, ML can unearth hidden patterns from data that aid scientists in understanding new mechanisms and links in QDs[17][23]. Predicting properties of QDs in diverse conditions using ML is important in materials design for specific applications[20].

All inorganic metal halide Perovskite Quantum Dots (PQDs) have shown great promise due to their unique optical and electronic properties. They exhibit size- and composition-dependent properties and are cubic in shape, with the size ranging from approximately 3 nm to 15 nm. Therefore, PQDs offer band gap tunability over a wide range and property tailoring capabilities. Compared to their counterparts, PQDs have high photoluminescence quantum yield, narrow emission linewidth, higher stability, higher charge mobility, and longer diffusion length [5][24][22][2][21]. These properties make them exceptionally critical in a wide range of applications; including solar cells[26], lasers[21], LEDs[6], and medical imaging[16]. PQDs are produced using the colloidal synthesizing method at high temperatures where the temperature, reaction time, and the amount of substance are significantly vital for the properties of PQDs. Therefore, to obtain PQDs with the anticipated optical and electronic properties, it is necessary to carefully design the experiment conditions with the full knowledge of every parameter's effect. This process is usually carried out by trial and error, which is time-consuming, costly and requires intensive manpower. In this context, ML is a powerful tool to predict the precise conditions of experiments for synthesizing PQDs with the desired properties. It has been shown that ML enables researchers to extract valuable insights from large datasets such as forecasting a variety of chemical and physical features of materials to find intricate mathematical relationships within empirical data [9]. Different ML algorithms have been applied to the synthesizing conditions of several QDs to predict their sizes including, CdSe[1], PbSe[1], ZnSe [1], InP[11] and ZnO[13] QDs. However, a comprehensive ML study has not been conducted to predict the optical properties of PQDs yet.

In this work, we applied several ML algorithms to predict the output properties of CsPbCl₃ PQDs synthesized via the hot-injection method. Based on the predicted photoluminescence, absorption and size properties of CsPbCl₃ PQDs, we compared the performances of ML models of SVR, NND, Deep Learning, Decision Tree, Random Forest, and GBM.

2 METHODOLOGY

2.1 Data Description

We initiated our research by thoroughly analysing existing literature to compile a comprehensive database of hot injection synthesis parameters for CsPbCl₃

PQDs. The data was collected from a total of 59 peer-reviewed articles which are listed in Table S1 in the supporting information section. Once the selected papers were decided, relevant synthesis parameters and the corresponding output properties were extracted manually. The following parameters are considered as the independent input variables to train algorithms; The injection temperature, the source of chloride (Cl), the amount of Cl in millimoles (mmol), the source of lead (Pb), the amount of Pb in mmol, the cesium (Cs) source, the quantity of Cs in mmol, the molar ratio of Cs-to-Pb, and the molar ratio of Cl to Pb. In addition, the quantities of octadecene (ODE), oleic acid (OA), and oleylamine (OLA) in millilitres (ml), along with the total volume of ligands (OA+OLA) in ml, are also included as input parameters. Furthermore, the ratio of Cl amount to total ligand volume and the amount of Pb to total ligand volume are also utilised as input features. The output target parameters are PQDs' size in nanometer (nm), the 1S abs peak in nm and the PL in nm. We suitably classified the collected data, each variable parameter located in its respective columns, and every outcome in its respective rows. This well-ordered records set improved the model better trained and quicker in data management.

2.2 Machine Learning Models and Metrics

The dataset is separated into training and testing categories according to the hierarchical clustering framework instead of using the same ones repetitively to avoid cases where memorizing or overfitting hinders new information. We evaluated the six regression methods that are suitable for small datasets: SVR, NND, DL, DT, RF and GBM. All of these algorithms were built using the sklearn library. To guarantee representative samples for testing and training, we utilised both random sampling and stratified sampling techniques. We partitioned our data sets into training which contained 80% examples while testing contains the remaining 20% examples. The tuning hyperparameters were performed through Grid search. We evaluated the model's performance by computing R^2 , MAE and RMSE metrics. MAE mainly considers outliers and compares datasets, and models with different objectives measured on the scale. A simple way to visualise the model's performance is to look at its MAE value; lower values correspond to higher predicted accuracy. The distance between the predicted actual value and the observed value of the data sample is the best way to interpret RMSE. If RMSE equals zero, then the model is correctly estimating all prices. The coefficient of determination noted as R^2 is a metric that quantifies the degree to which the model accurately represents the data, with values closer to 1 suggesting a higher level of accuracy.

In data science, SVR is a line of regression model that is effective in modeling complex relationships within a dataset through the mapping of input data into a higher dimensional space. SVR's application is of importance especially in dealing with high-dimensional data sets and not-linear relationships. Which can make SVR computationally intensive especially with large datasets The SVR model was created using the radial basis function (RBF) kernel with the scikit-learn Python module. The hyperparameters were optimised using a grid search technique.

NND is an important concept in spatial analysis and machine learning. More

precisely, it plays a significant role in pattern recognition as well as classification algorithms which includes k-Nearest Neighbor (k-NN) method. NND is defined as the shortest length that separates any two points within the dataset from one another. NND has been applied in computational geometry foundational concepts, particle systems theoretical analysis, and statistical estimator convergence analysis, according to [7]. The Python scikit-learn library was also utilised to implement the NND model.

DT are straightforward but robust models that are simple to understand and illustrate. They can deal with both numerical and categorical data, hence becoming flexible for diverse data sets. Nevertheless, decision trees are susceptible to overfitting specifically as the tree becomes too deep. To train the model, a decision tree model was developed using Python's scikit-learn module. The model's parameters, including its maximum depth, were changed by applying cross-validation.

RF is a machine learning algorithm that has become famous in recent days [27]. It is considered one of the best machine learning algorithms by many people because: it can handle a thousand variables without compromising the accuracy; it is fast; it is simple to implement; and its prediction accuracy is high [18]. This algorithm has been referred to as one with high-level prediction performance but requiring less tuning hence regarded as the most appropriate out-of-the-box classification and regression algorithm [14]. The RF model was implemented in Python's scikit-learn module. 500 trees were used to train the model, and cross-validation was used to optimise `max_features`, the number of features to take into account at each split.

GBM is another machine learning technique that is significantly strong because it combines many weak learners. This technique is efficient in many classification tasks [3]. It has also been identified for its high predictive accuracy and effectiveness when working with complicated interactions in the data. However, it tends to overfit when not well-adjusted as one of the drawbacks of GBM. Python was used to train the GBM model with the scikit-learn library. By implementing cross-validation on critical parameters such as learning rate, number of boosting rounds and `max_depth`, they were properly optimized.

DL, particularly neural networks, possess the potential to learn through examples in the same way humans do. These networks do not require specific algorithms and are capable of estimating any nonlinear transformation; hence they can be used to determine inputs/outputs for intricate systems [25]. Nonetheless, there are problems associated with using older model architectures that include a lack of balance within the dataset resulting in memorization rather than generalization by machine learning algorithms themselves as well as redundancy within feature extraction along with ignoring cross-layer characteristic interactions [10]. We used scikit-learn library for training our RF model in Python.

3 RESULTS AND DISCUSSION

The numerical simulations performed in this study have given a more detailed account of how well machine learning techniques could forecast the Size, 1S abs

and PL for CsPbCl₃ PQDs. The employed models were SVR, NND, DT, RF, GBM and DL. For training and testing data sets, standard measures like RMSE, MAE and R² were used in order to assess the models's performance levels. A series of numerical experiments have given us a full and clear understanding of forecasting CsPbCl₃ PQDs' size, 1S abs and PL output through the indicated ML models.

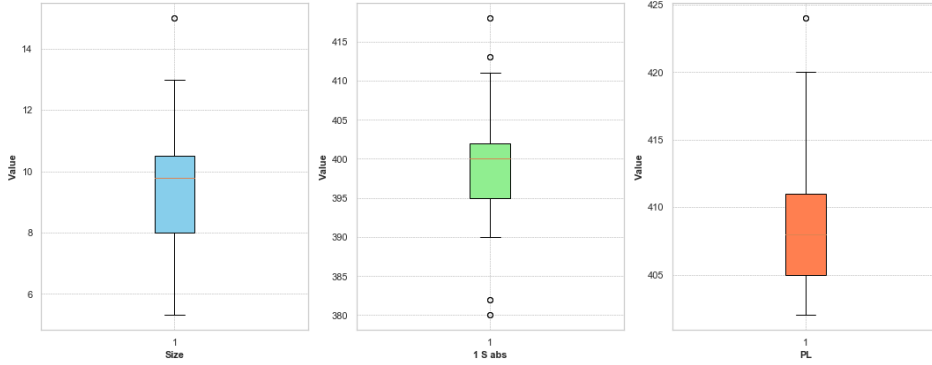


Figure 1: Box plots for the Size, 1S abs, PL providing the data distribution, median, quartiles, and potential outliers for each variable.

Initially, to identify the distribution of the data collected from the papers, the outlier data, and data medians, we generated the boxplot for the three output properties as shown in Figure 1. It is seen that the median size distribution of PQDs is around 9.5 nm, whereas the 1S abs and PL ranges vary between 395 and 402 nm and 405 and 412 nm, respectively. Next, to compare the actual and predicted processed values using ML algorithms, we conducted scatter graphs of all models for three output properties of CsPbCl₃ PQDs. Figure 2 compares the DT model prediction against actual values of size, 1S abs and PL outputs. Clearly, it shows how accurate the model performs. The predicted and observed values for three output properties of PQDs are almost overlapped in this model. Test data RMSE values of as low as 0.23, 0.19 and 0.16 are respectively obtained for size, 1S abs and PL in this algorithm. On the other hand, the minimum test data MAE indicators of 0.16, 0.13 and 0.11 are calculated for the properties of size, 1S abs and PL, respectively. Similar Scatter graphs for other employed ML algorithms are given in Figures S1,2,3,4,5 in the supporting information section. These models also yielded similar prediction performances for properties of CsPbCl₃ PQDs. All these findings suggest that ML algorithms are powerful tools for estimating the properties of PQDs accurately.

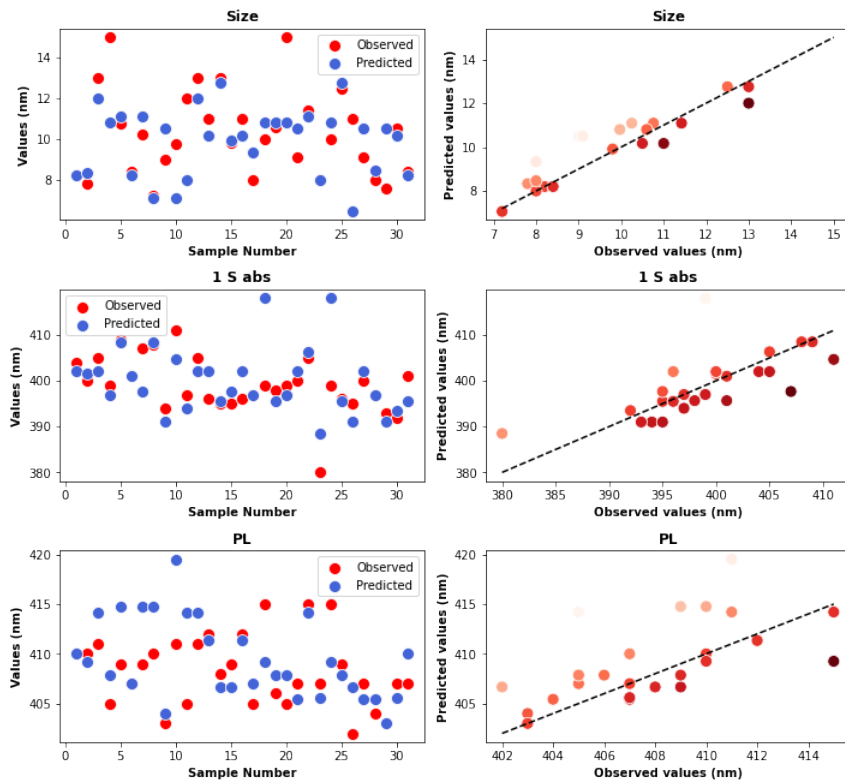


Figure 2: Parity plots of predicted vs. observed values for the Size, 1S abs and PL outputs of the CsPbCl₃ PQDs using DT regression model

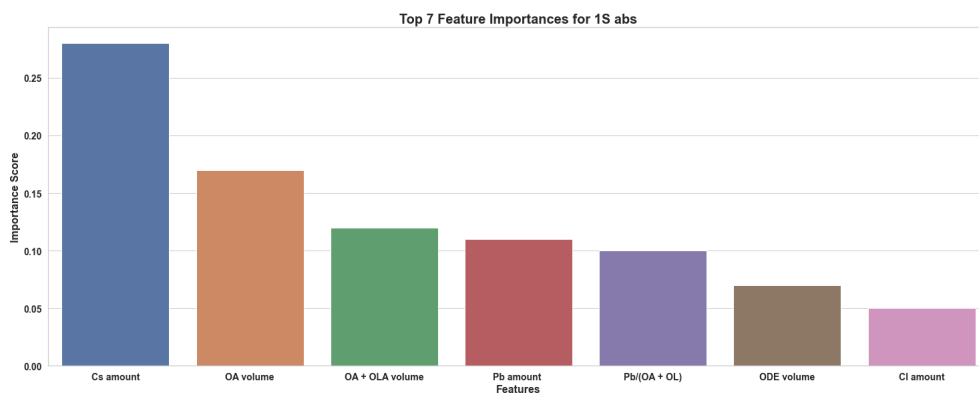


Figure 3: Importance of the variables for 1S abs using the RF regression model.

Table 1: Comparison of performance metrics values for Size, 1S abs, and PL using all ML methods.

	Model	Train data			Test data		
		R ²	RMSE	MAE	R ²	RMSE	MAE
Size	SVR	0.99	0.009	0.009	0.80	0.34	0.16
	NND	0.99	0.012	0.008	0.62	0.47	0.30
	Deep Learning	0.77	0.49	0.38	0.10	0.74	0.56
	Decision Tree	0.94	0.23	0.17	0.94	0.23	0.16
	Random Forest	0.93	0.26	0.20	0.51	0.66	0.54
	GBM	0.97	0.14	0.13	0.48	0.56	0.38
1 S abs	SVR	0.99	0.009	0.008	0.84	0.34	0.19
	NND	0.99	0.009	0.005	0.55	0.59	0.34
	Deep Learning	0.66	0.59	0.39	0.44	0.66	0.49
	Decision Tree	0.96	0.19	0.13	0.96	0.19	0.13
	Random Forest	0.94	0.23	0.17	0.64	0.53	0.37
	GBM	0.98	0.11	0.09	0.66	0.51	0.30
PL	SVR	0.99	0.009	0.009	0.66	0.58	0.28
	NND	0.99	0.005	0.002	0.78	0.46	0.29
	Deep Learning	0.73	0.51	0.38	0.53	0.68	0.56
	Decision Tree	0.97	0.16	0.11	0.97	0.16	0.11
	Random Forest	0.94	0.23	0.16	0.70	0.54	0.39
	GBM	0.99	0.09	0.07	0.71	0.53	0.34

The input feature importance for predicting 1S abs using the RF algorithm is shown in Figure 3. The amounts of Cs and OA are seen to be the most significant features, whereas the quantity of Cl and ODE are found to be the less important input features for accurately estimating the indicated property. On the other hand, for size and PL outputs the amounts of Pb and Cs are the most significant input parameters, respectively (See Figures S8 & S9).

To minimize the similarity for the training and test data, we compared R², RMSE, and MAE metrics obtained from test and trained data for 1S abs target output for all employed algorithms, as shown in Figure 4. The training data and the testing data appear in different parts of the bar plots. Overall, SVR and NND could perform better than other algorithms for training data, whereas, for test data SVR and DT models outperform their rivals. The metric performance comparison for size and PL outputs of the CsPbCl₃ PQD can be seen in Figures S6 and S7 in the supporting information section.

The Table 1 compiles the metric (R², RMSE, and MAE) performances of training and test data set for three target parameters of CsPbCl₃ PQDs using all ML models. In general, all used ML algorithms utilised in this study provide high accuracy for predicting the target characteristics. The SVR model yields the highest R² values for three target features in the test data category compared with the other models, which is an indicator of being the most accurate prediction method. In this model, in the trained data category, the RMSE and MAE metrics are found to be as low as 0.009, which gives one of the best accuracy among all prediction models. These observations also agree with the results obtained from Figure S5 for three outputs, where the predicted and observed values are well-correlated. On the other hand, the NND model is also found to

be as accurate as the SVR model. It is obvious that the metrics performances of NND model are nearly identical to those of the SVR model. The well data arrangement in Figure S1 for size, 1S abs, and PL properties of the PQDs, also confirms the accuracy of the NND model.

Conversely, DL and RF models seem to be the least accurate method for predicting the properties of CsPbCl₃ PQDs. For example, the RMSE and MAE metrics values for predicting test data set for size feature are 0.74 and 0.56, respectively, being 2 times and 3 times lesser those of the SVR model. Although the prediction performance of RF and DL for size feature are inferior to others employed in this study, their performances are marginally better than that used for different QDs in the literature [1]. The metrics values for all target parameters obtained from GBM and DT models demonstrate a moderate performance between the SVR-NND and DL-RF algorithm couples. These two models showed better prediction performance when used for PL output estimation.

A Pearson correlation heatmap is a graphical representation that effectively communicates the Pearson correlation coefficients (ranging between -1 to +1) among variables within a dataset. The heatmap displays a colour-coded matrix, with warmer colours indicating stronger positive correlations, cooler colours representing stronger negative correlations, and neutral colours signifying no link between variables [12]. Figure 5 shows the Pearson correlation heatmap to demonstrate the correlations between the input and output parameters dataset of CsPbCl₃ PQDs. 1S abs and PL have a positive correlation of 0.66, whereas, the correlations between size and PL and size and 1S abs are considerably inferior.

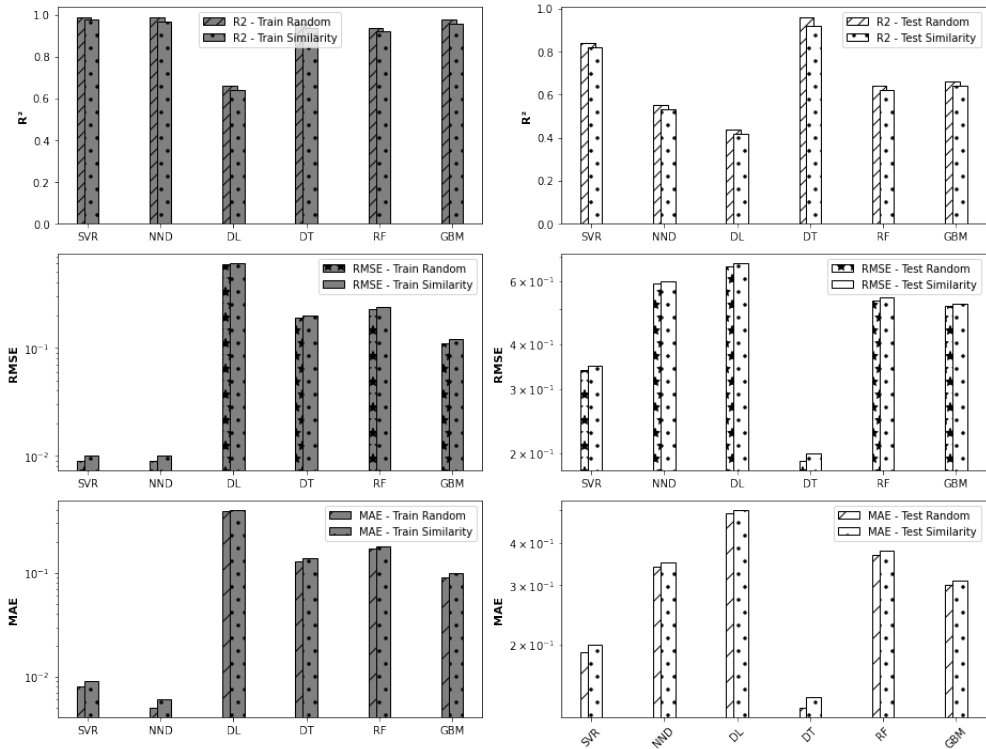


Figure 4: Performance metrics for the algorithm trained and tested in 1S abs output, with splitting based on random conditions or to minimize similarity for the training and test data.

From synthesis parameters, results have shown that machine learning can be used to accurately predict the properties of CsPbCl₃ quantum dots. In fact, the most efficient ones were SVR and RF models which performed well in their predictions and also provided some guidance in understanding the parameters affecting the properties of quantum dots. The importance of growth temperature was underlined by RF because these variables have a direct effect on quantum dots characteristics and hence require precise control measures. Another finding was that; NND and DT models though fast at producing easily understood outputs might need further optimization if they are to match other sophisticated models like GBM or DL. Boxplots and correlation analyses serve as an additional level of validation for ensuring predictive model stability. In general, this paper demonstrates how ML can help in the control and synthesis of QDs implying a route to more efficient experimental designs.

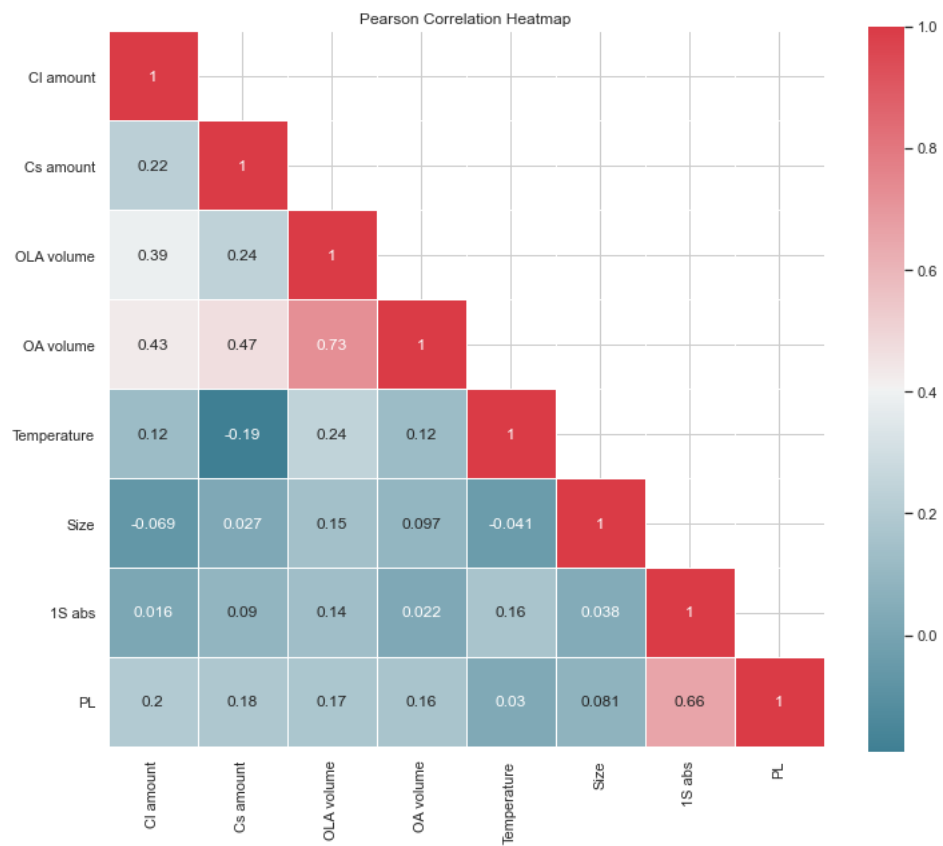


Figure 5: Pearson correlation shows a strong correlation between the three output targets

4 CONCLUSION

This study aimed to predict the size, 1S abs and PL properties of CsPbCl₃ PQDs by comparing the performances of ML algorithms of SVR, NND, GBM, RF, DT and DL. Generally, nearly all models succeeded in promising outcomes in predicting the outputs of PQDs. Among them, SVR and NND models indicated the best performance as they make accurate predictions and give insights into factors that affect QD properties. The SVR and NND ML models demonstrate RMSE metric values of 0.009 and 0.012 for the train data, and 0.34 and 0.47 for the test data, respectively. These findings are close to actual data, which indicate that the employed ML models have the capability of predicting properties of CsPbCl₃ PQDs with high accuracy. For the future direction, the results suggest that the progress of ML can significantly contribute to the progress of QDs design, resulting in more tailored QDs with specific properties.

Supporting Information

Electronic supporting information (ESI) is accessible: Additional details about the similarity between the training and test data, the significance of the variables in terms of feature importance, and the comparison of predicted and observed outputs of the CsPbCl₃ PQDs and compound databases.

Acknowledgements

References

- [1] Fábio Baum, Tatiane Pretto, Ariadne Köche, and Marcos José Leite Santos. Machine learning tools to predict hot injection syntheses outcomes for ii–vi and iv–vi quantum dots. *The Journal of Physical Chemistry C*, 124(44):24298–24305, 2020.
- [2] Jonathan De Roo, Maria Ibáñez, Pieter Geiregat, Georgian Nedelcu, Willem Walravens, Jorick Maes, Jose C Martins, Isabel Van Driessche, Maksym V Kovalenko, and Zeger Hens. Highly dynamic ligand binding and light absorption coefficient of cesium lead bromide perovskite nanocrystals. *ACS nano*, 10(2):2071–2081, 2016.
- [3] Manqing Dong, Lina Yao, Xianzhi Wang, Boualem Benatallah, and Shuai Zhang. Grcan: gradient boost convolutional autoencoder with neural decision forest. *arXiv preprint arXiv:1806.08079*, 2018.
- [4] Yasemin Gündoğdu, Hamdi Şükür Kılıç, and Musa Çadırcı. Third order nonlinear optical properties of cdte/cdse quasi type-ii colloidal quantum dots. *Optical Materials*, 114:110956, 2021.
- [5] He Huang, Maryna I Bodnarchuk, Stephen V Kershaw, Maksym V Kovalenko, and Andrey L Rogach. Lead halide perovskite nanocrystals in the research spotlight: stability and defect tolerance. *ACS energy letters*, 2(9):2071–2083, 2017.
- [6] Yun-Fei Li, Jing Feng, and Hong-Bo Sun. Perovskite quantum dots for light-emitting devices. *Nanoscale*, 11(41):19119–19139, 2019.
- [7] Elia Liitiäinen, Amaury Lendasse, and Francesco Corona. Bounds on the mean power-weighted nearest neighbour distance. *Proceedings of the Royal Society A: Mathematical, Physical and Engineering Sciences*, 464(2097):2293–2301, 2008.
- [8] Yuan Liu, Ayush Jain, Clara Eng, David H Way, Kang Lee, Peggy Bui, Kimberly Kanada, Guilherme de Oliveira Marinho, Jessica Gallegos, Sara Gabriele, et al. A deep learning system for differential diagnosis of skin diseases. *Nature medicine*, 26(6):900–908, 2020.
- [9] Yu-Chen Lo, Stefano E Rensi, Wen Tornø, and Russ B Altman. Machine learning in chemoinformatics and drug discovery. *Drug discovery today*, 23(8):1538–1546, 2018.
- [10] Xiaopu Ma, Jiangdan Shan, Fei Ning, Wentao Li, and He Li. Effnet: A skin cancer classification model based on feature fusion and random forests. *Plos one*, 18(10):e0293266, 2023.
- [11] Hao A Nguyen, Florence Y Dou, Nayon Park, Shenwei Wu, Harrison Sarsito, Benedicte Diakubama, Helen Larson, Emily Nishiwaki, Micaela Homer, Melanie Cash, et al. Predicting indium phosphide quantum dot properties from synthetic procedures using machine learning. *Chemistry of Materials*, 34(14):6296–6311, 2022.

- [12] Clare Rainey, Angelina T Villikudathil, Jonathan McConnell, Ciara Hughes, Raymond Bond, and Sonyia McFadden. An experimental machine learning study investigating the decision-making process of students and qualified radiographers when interpreting radiographic images. *PLOS Digital Health*, 2(10):e0000229, 2023.
- [13] Paul Rossener Regonia, Christian Mark Pelicano, Ryosuke Tani, Atsushi Ishizumi, Hisao Yanagi, and Kazushi Ikeda. Predicting the band gap of zno quantum dots via supervised machine learning models. *Optik*, 207:164469, 2020.
- [14] Jake S Rhodes, Adele Cutler, and Kevin R Moon. Geometry-and accuracy-preserving random forest proximities. *IEEE Transactions on Pattern Analysis and Machine Intelligence*, 2023.
- [15] Stuart J Russell and Peter Norvig. *Artificial intelligence: a modern approach*. Pearson, 2016.
- [16] Ilhwan Ryu, Jee-Yeon Ryu, Geunpyo Choe, Hyemin Kwon, Hyeji Park, Young-Seok Cho, Rose Du, and Sanggyu Yim. In vivo plain x-ray imaging of cancer using perovskite quantum dot scintillators. *Advanced Functional Materials*, 31(34):2102334, 2021.
- [17] Benjamin Sanchez-Lengeling and Alán Aspuru-Guzik. Inverse molecular design using machine learning: Generative models for matter engineering. *Science*, 361(6400):360–365, 2018.
- [18] Nilam Novita Sari, Ismaini Zain, Kartika Fithriasari, and Amri Muhaimin. Br+ for addressing imbalanced multilabel data classification combined with resampling technique. In *AECon 2020: Proceedings of The 6th Asia-Pacific Education And Science Conference, AECon 2020, 19-20 December 2020, Purwokerto, Indonesia*, page 421. European Alliance for Innovation, 2021.
- [19] Andrew W Senior, Richard Evans, John Jumper, James Kirkpatrick, Laurent Sifre, Tim Green, Chongli Qin, Augustin Žídek, Alexander WR Nelson, Alex Bridgland, et al. Improved protein structure prediction using potentials from deep learning. *Nature*, 577(7792):706–710, 2020.
- [20] Huachen Tao, Tianyi Wu, Matteo Aldeghi, Tony C Wu, Alán Aspuru-Guzik, and Eugenia Kumacheva. Nanoparticle synthesis assisted by machine learning. *Nature reviews materials*, 6(8):701–716, 2021.
- [21] Yue Wang, Xiaoming Li, Jizhong Song, Lian Xiao, Haibo Zeng, and Handong Sun. All-inorganic colloidal perovskite quantum dots: a new class of lasing materials with favorable characteristics. *Advanced materials*, 27(44):7101–7108, 2015.
- [22] Kaifeng Wu, Guijie Liang, Qiongyi Shang, Yueping Ren, Degui Kong, and Tianquan Lian. Ultrafast interfacial electron and hole transfer from cspbbr₃ perovskite quantum dots. *Journal of the American Chemical Society*, 137(40):12792–12795, 2015.

- [23] Zhenpeng Yao, Benjamín Sánchez-Lengeling, N Scott Bobbitt, Benjamin J Bucior, Sai Govind Hari Kumar, Sean P Collins, Thomas Burns, Tom K Woo, Omar K Farha, Randall Q Snurr, et al. Inverse design of nanoporous crystalline reticular materials with deep generative models. *Nature Machine Intelligence*, 3(1):76–86, 2021.
- [24] Gurivi Reddy Yettapu, Debnath Talukdar, Sohini Sarkar, Abhishek Swarnkar, Angshuman Nag, Prasenjit Ghosh, and Pankaj Mandal. Terahertz conductivity within colloidal cspbbr3 perovskite nanocrystals: remarkably high carrier mobilities and large diffusion lengths. *Nano letters*, 16(8):4838–4848, 2016.
- [25] Ningrui Zhao and Jinwei Lu. Review of neural network algorithm and its application in temperature control of distillation tower. *Journal of Engineering Research and Reports*, 20(4):50–61, 2021.
- [26] Qian Zhao, Abhijit Hazarika, Xihan Chen, Steve P Harvey, Bryon W Larson, Glenn R Teeter, Jun Liu, Tao Song, Chuanxiao Xiao, Liam Shaw, et al. High efficiency perovskite quantum dot solar cells with charge separating heterostructure. *Nature communications*, 10(1):2842, 2019.
- [27] Yangming Zhou and Guoping Qiu. Random forest for label ranking. *Expert systems with applications*, 112:99–109, 2018.

Supporting Information

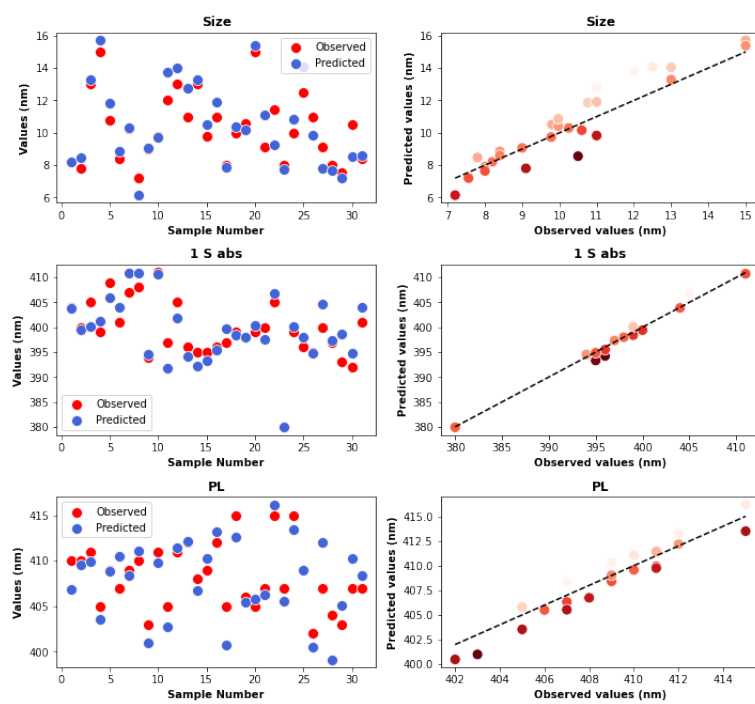


Figure S1: Predicted vs. observed plot of the NND regression model for the Size, 1S abs and PL outputs of the CsPbCl₃ PQDs.

Table S1: DOIs are utilised to consolidate the databases.

CsPbCl ₃ Database DOIs			
01.	10.1002/adfm.202100930	02.	10.1016/j.jlumin.2021.118658
03.	10.1021/acsenergylett.8b01441	04.	10.1021/acsnano.8b07850
05.	10.1016/j.solener.2020.05.070	06.	10.1016/j.optmat.2022.113362
07.	10.1016/j.materresbull.2018.12.004	08.	10.1007/s00339-022-05962-7
09.	10.1021/acsenergylett.9b02678	10.	10.1021/acs.jpcclett.8b03047
11.	10.1021/acsmaterialslett.9b00101	12.	10.1021/acs.chemmater.9b05082
13.	10.1016/j.matchemphys.2021.125479	14.	10.1039/D0RA09043C
15.	10.1021/acs.nanolett.6b02772	16.	10.1021/jacs.6b08085
17.	10.1021/acs.jpcclett.1c02416	18.	10.1021/acs.jpcc.8b06579
19.	10.1021/acs.chemmater.8b02157	20.	10.1021/acs.jpcc.8b11906
21.	10.1021/acs.jchemed.8b00735	22.	10.1021/acsenergylett.8b01909
23.	10.1021/acsanm.0c01254	24.	10.1021/acs.jpcc.8b12035
25.	10.1039/C7RA06597C	26.	acsanm.1c01623
27.	10.1021/acsenergylett.7b00375	28.	10.1039/C8NR10439E
29.	10.1016/j.nanoen.2018.06.073	30.	10.1002/asia.202200478
31.	10.1016/j.nanoen.2020.105163	32.	10.1021/acs.jpcc.1c04335
33.	10.1021/acs.jpcc.7b06929	34.	10.1038/srep45906
35.	10.1039/C9RA05685H	36.	10.1016/j.jallcom.2019.02.032
37.	10.1039/C9RA07069A	38.	10.1021/acs.nanolett.5b02404
39.	10.1021/acs.jpcc.6b12828	40.	10.1021/acs.chemmater.9b05082
41.	10.1016/j.materresbull.2020.110907	42.	10.1039/c8tc03957g
43.	10.1039/C8TC03139H	44.	10.1063/1.5127887
45.	10.1039/c7nr08136g	46.	10.1088/2632-959X/abcf8e
47.	10.1039/d1nr04455a	48.	10.1016/j.ceramint.2022.07.310
49.	10.1021/acsanm.3c01960	50.	10.1039/c7nr06745c
51.	10.1021/acs.jpcc.1c06995	52.	10.1021/acs.chemmater.0c01325
53.	10.1021/acs.jpcclett.9b03831	54.	10.1021/acsenergylett.0c00931
55.	10.1021/acsami.8b14046	56.	10.1021/acs.nanolett.7b04575
57.	10.1016/j.ceramint.2022.09.075	58.	10.1021/acs.jpcclett.1c00017
59.	10.1016/j.jallcom.2021.161505	60.	

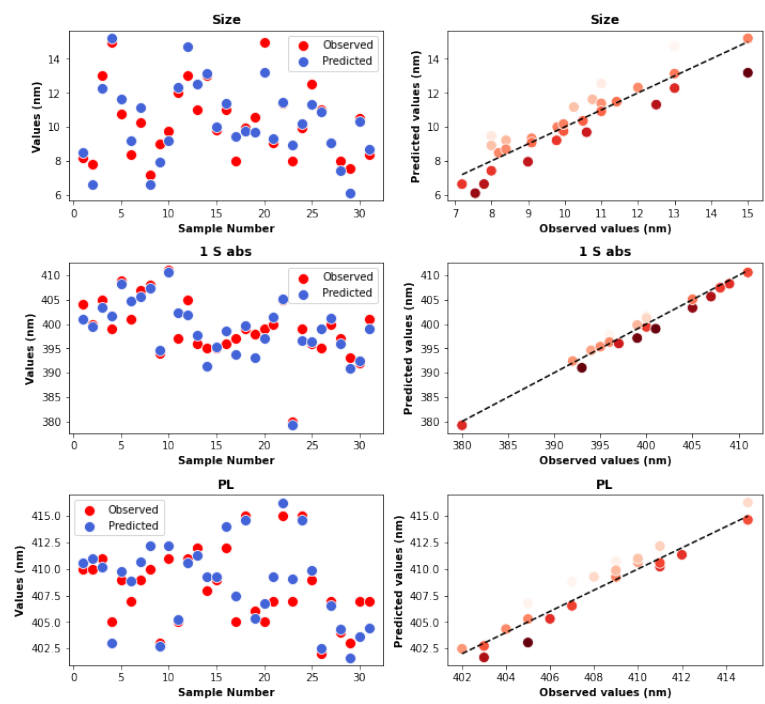


Figure S2: Predicted vs. observed plot of the RF regression model for the Size, 1S abs and PL outputs of the CsPbCl₃ PQDs.

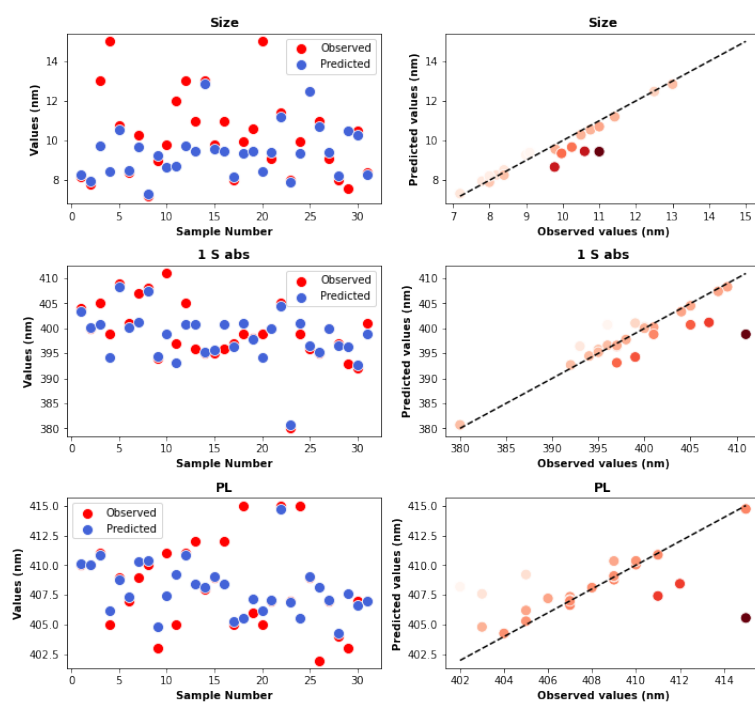


Figure S3: Predicted vs. observed plot of the GBM regression model for the Size, 1S abs and PL outputs of the CsPbCl₃ PQDs.

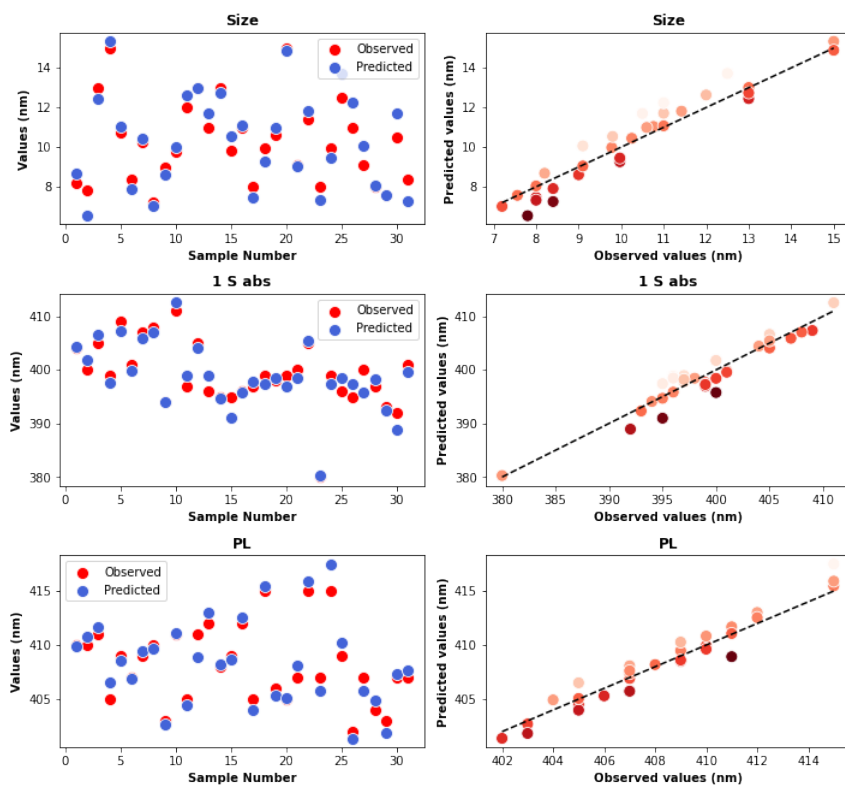


Figure S4: Predicted vs. observed plot of the DL regression model for the Size, 1S abs and PL outputs of the CsPbCl₃ PQDs.

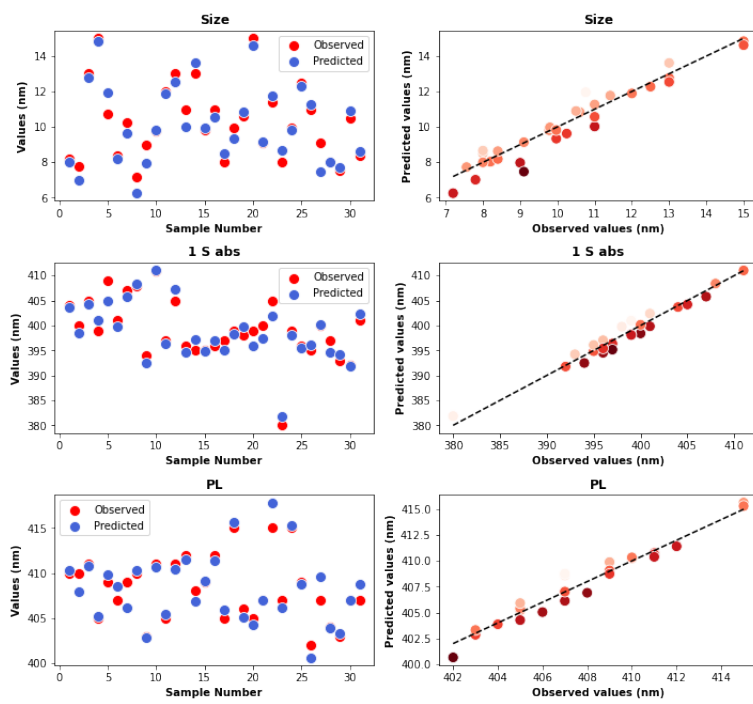


Figure S5: Predicted vs. observed plot of the SVR model for the Size, 1S abs and PL outputs of the CsPbCl₃ PQDs.

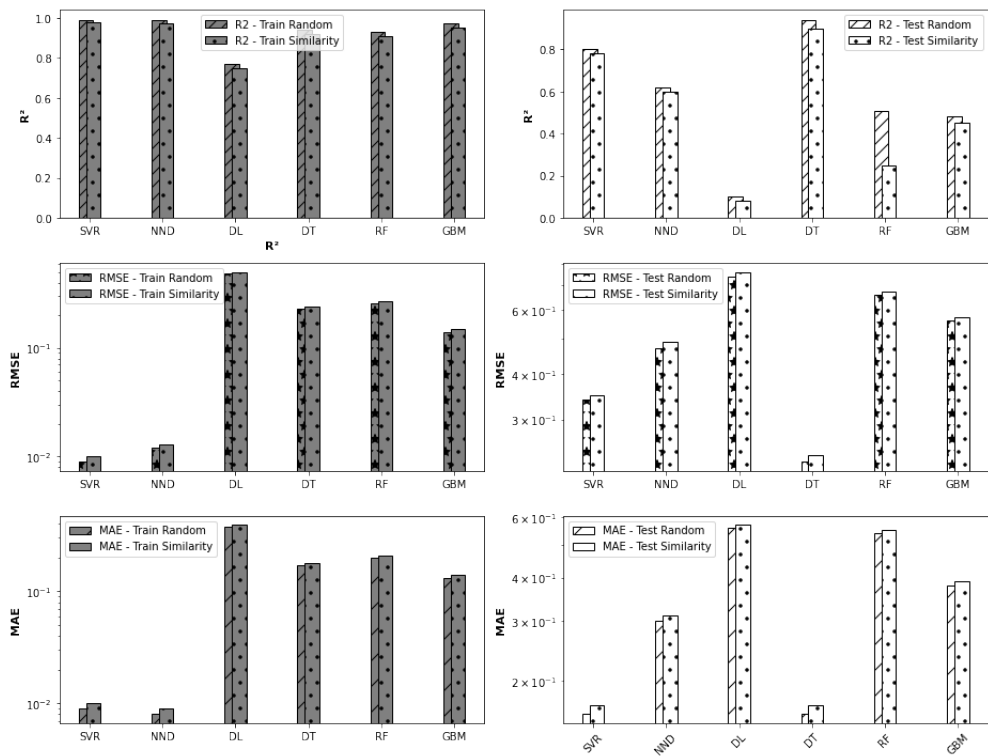


Figure S6: Performance metrics for the the algorithm trained and tested in Size output, with splitting based on random conditions or to minimize similarity for the training and test data.

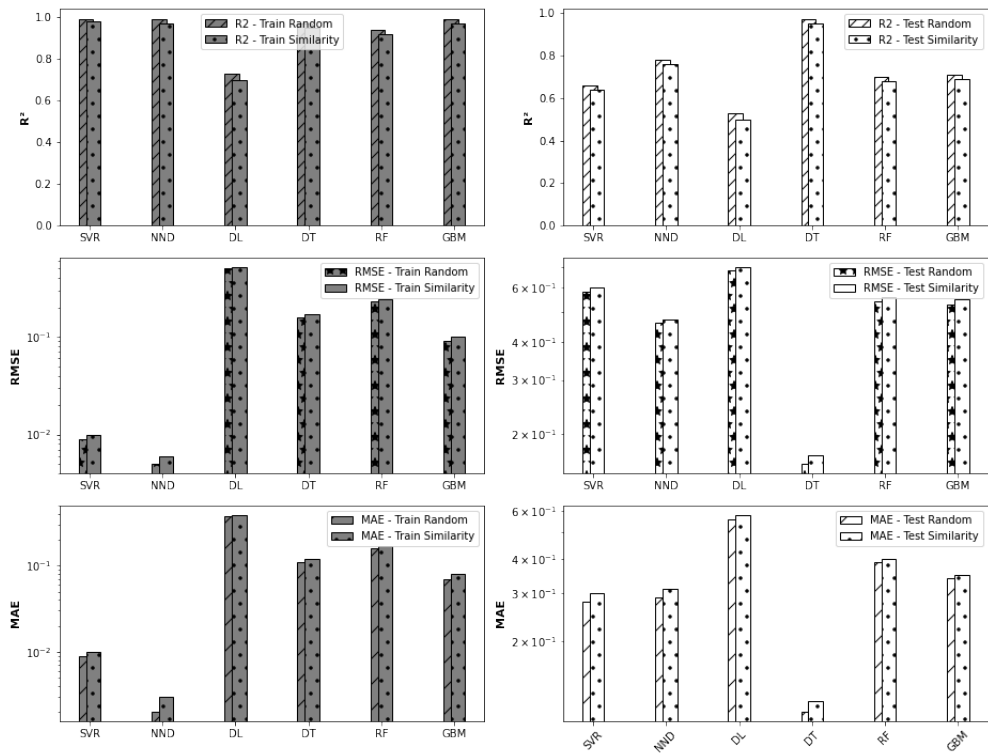


Figure S7: Performance metrics for the algorithm trained and tested in PL output, with splitting based on random conditions or to minimize similarity for the training and test data.

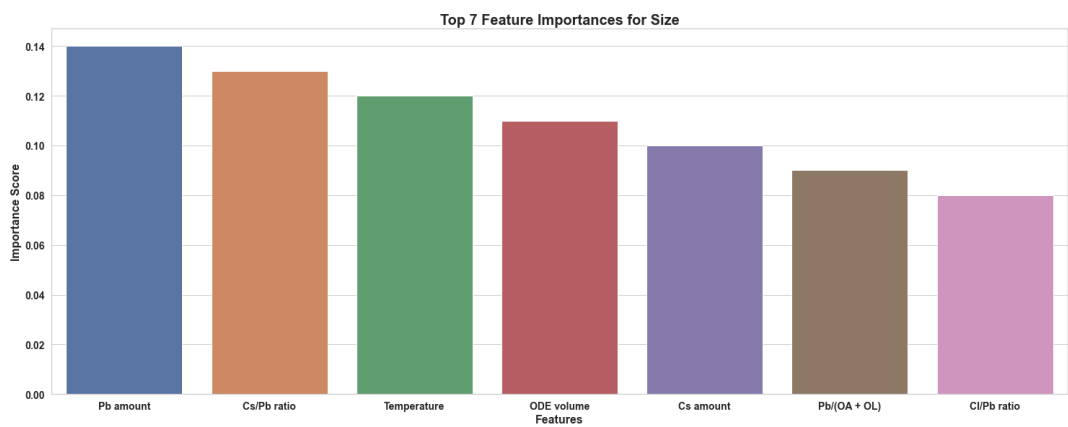


Figure S8: Importance of the variables for Size using the RF regression model.

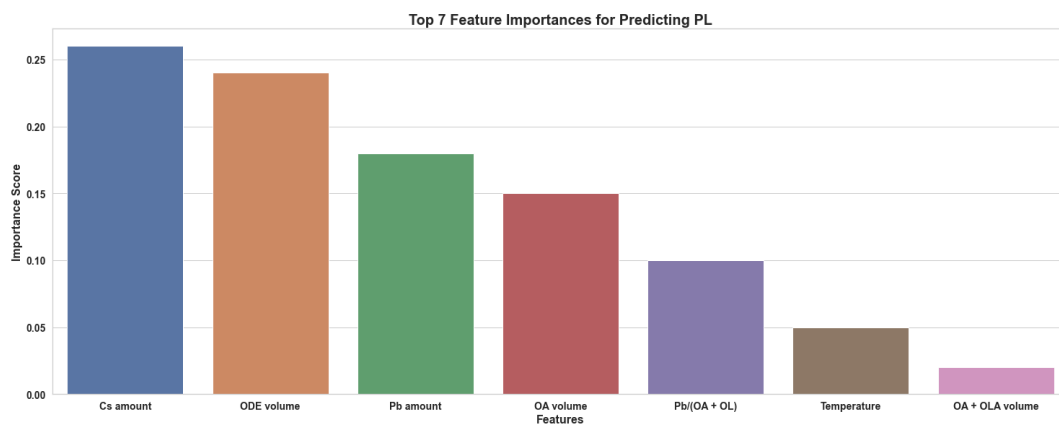


Figure S9: Importance of the variables for PL using the RF regression model.